0022-3565/11/3372-503–512$25.00
THE JOURNAL OF PHARMACOLOGY AND EXPERIMENTAL THERAPEUTICS
JPET 337:503–512, 2011

Vol. 337, No. 2
177220/3682875
Printed in U.S.A.

Mechanisms Underlying Differences in Systemic Exposure of Structurally Similar Active Metabolites: Comparison of Two Preclinical Hepatic Models[S]

Grace Zhixia Yan, Kim L. R. Brouwer, Gary M. Pollack, Michael Zhuo Wang, Richard R. Tidwell, James E. Hall, and Mary F. Paine

Division of Pharmacotherapy and Experimental Therapeutics, UNC Eshelman School of Pharmacy (G.Z.Y., K.L.R.B., G.M.P., M.Z.W., M.F.P.) and Department of Pathology and Laboratory Medicine, School of Medicine (R.R.T., J.E.H.), University of North Carolina, Chapel Hill, North Carolina

Received November 12, 2010; accepted February 7, 2011

ABSTRACT

Selection of in vitro models that accurately characterize metabolite systemic and hepatobiliary exposure remains a challenge in drug development. In the present study, mechanisms underlying differences in systemic exposure of two active metabolites, furamidine and 2,5-bis (5-amidino)-2-pyridyl furan (CPD-0801), were examined using two hepatic models from rats: isolated perfused livers (IPLs) and sandwich-cultured hepatocytes (SCH). Pafuramidine, a prodrug of furamidine, and 2,5-bis [5-(*N*-methoxyamidino)-2-pyridyl] furan (CPD-0868), a prodrug of CPD-0801, were selected for investigation because CPD-0801 exhibits greater systemic exposure than furamidine, despite remarkable structural similarity between these two active metabolites. In both IPLs and SCH, the extent of conversion of CPD-0868 to CPD-0801 was consistently higher than that of pafuramidine to furamidine over time (at most 2.5-fold); area under the curve (AUC) of CPD-0801 in IPL perfusate and SCH medium was at least 7-fold higher than that of furamidine. Pharmacokinetic modeling revealed that the rate constant for basolateral (liver to blood) net efflux ($k_{A\_net\ efflux}$) of total formed CPD-0801 (bound + unbound) was 6-fold higher than that of furamidine. Hepatic accumulation of both active metabolites was extensive (>95% of total formed); the hepatic unbound fraction ($f_{u,L}$) of CPD-0801 was 5-fold higher than that of furamidine (1.6 versus 0.3%). Incorporation of $f_{u,L}$ into the pharmacokinetic model resulted in comparable $k_{A\_net\ efflux,u}$ between furamidine and CPD-0801. In conclusion, intrahepatic binding markedly influenced the disposition of these active metabolites. A higher $f_{u,L}$ explained, in part, the enhanced perfusate AUC of CPD-0801 compared with furamidine in IPLs. SCH predicted the disposition of prodrug/metabolite in IPLs.

Introduction

The liver often is the predominant organ for biotransformation of a precursor compound (i.e., prodrug) to active metabolite, which can influence therapeutic and/or toxicological outcomes (Pang et al., 2008). Once formed, active metabolite can undergo further metabolism, excretion into the systemic circulation or bile, and/or intrahepatic sequestration. Therefore, accurate characterization of the systemic and hepatobiliary exposure of active metabolite is imperative for efficacy and risk assessment. Although physiologically relevant, in vivo studies are cumbersome, costly, and associated with a variety of extrahepatic variables, including metabolic and active uptake/efflux processes in the intestine and kidney. As an alternative methodology, in vitro or ex vivo hepatic models that have strong descriptive and predictive capabilities for the in vivo situation would offer significant advantages.

Isolated perfused livers (IPLs) are considered the closest approximation to the hepatobiliary system in vivo because of maintenance of hepatic architecture, microcirculation, and bile production (Brouwer and Thurman, 1996). Biotransformation pathways, sinusoidal/biliary transport processes,

This work was supported by the National Institutes of Health National Institute of General Medical Sciences [Grants R01-GM41935, R25-GM74088] and the Consortium for Parasitic Drug Development. G.Z.Y. was supported by an Eli Lilly Predoctoral Fellowship in Pharmacokinetics and Drug Disposition.

Article, publication date, and citation information can be found at http://jpet.aspetjournals.org.

doi:10.1124/jpet.110.177220.

[S] The online version of this article (available at http://jpet.aspetjournals.org) contains supplemental material.

ABBREVIATIONS: CPD-0801, 2,5-bis (5-amidino)-2-pyridyl furan; CPD-0868, 2,5-bis [5-(*N*-methoxyamidino)-2-pyridyl] furan; HAT, human African trypanosomiasis; IPL, isolated perfused liver; SCH, sandwich-cultured hepatocytes; DMEM, Dulbecco's modified Eagle's medium; NEAA, nonessential amino acids; DEX, dexamethasone; HBSS, Hanks' balanced salt solution; PBS, phosphate-buffered saline; LDH, lactate dehydrogenase; AUC, area under the curve; BLQ, below the limit of quantification; DMSO, dimethyl sulfoxide; LC-MS/MS, liquid chromatography with detection by tandem mass spectrometry; HPLC, high-performance liquid chromatography.

mechanisms underlying drug-drug interactions, and alterations in physiology (blood flow or changes in protein binding that might be associated with disease) can be elucidated by manipulating experimental conditions, in the absence of extrahepatic influences. Despite these advantages, several shortcomings limit the widespread use of IPLs, such as the delicate surgical techniques required, the relatively short experimental period in which viability is maintained (≤2 h), and the time/labor-intensive nature of the procedure (Brouwer and Thurman, 1996).

Sandwich-cultured hepatocytes (SCH) have emerged as an alternative in vitro model of the hepatobiliary system (Swift et al., 2010). Unlike conventional culture, hepatocytes cultured between layers of gelled collagen in a sandwich configuration establish cell polarity and form intact canalicular networks with appropriate localization, expression, and function of transport proteins (LeCluyse et al., 1994; Liu et al., 1999a). Compared with IPLs, SCH represent a more cost-effective and high-throughput system, allowing for simultaneous monitoring of xenobiotics in both cells and culture medium over an extended period of time (up to 24 h). One limitation of SCH is that catalytic activity of cytochrome P450 enzymes declines with days in culture (Boess et al., 2003). A medium additive, dexamethasone (DEX), has been reported to induce the expression of certain phase I and II enzymes in SCH to levels that more closely approximate in vivo metabolic activity (LeCluyse, 2001; Hewitt et al., 2007a,b; Kienhuis et al., 2007).

A large body of literature describes the hepatobiliary disposition of many xenobiotics using IPLs or SCH. However, a comparison of both sinusoidal/canalicular transport and metabolism between these two hepatic models has not been evaluated. In the current study, two antiparasitic prodrugs and derived metabolites were used as model drug/metabolite pairs to investigate this unaddressed issue.

Human African trypanosomiasis (HAT), a neglected parasitic disease, consists of two stages. During first-stage infection, parasites are restricted to the hemolymphatic system; second-stage infection begins once parasites invade the central nervous system, causing serious neurologic dysfunction (Barrett, 2010). Without treatment, HAT is invariably fatal. Pafuramidine (Fig. 1), a prodrug of furamidine (Fig. 1), is the only orally active agent that has shown efficacy in clinical trials for the treatment of first-stage infection (Paine et al., 2010). 2,5-Bis [5-(*N*-methoxyamidino)-2-pyridyl] furan (CPD-0868) (Fig. 1), a structural analog of pafuramidine and prodrug of 2,5-bis (5-amidino)-2-pyridyl furan (CPD-0801) (Fig. 1), demonstrated a higher cure rate compared with pafuramidine in a second-stage mouse model (4/5 versus 1/5 at 50 mg/kg p.o. for 10 days) (Wenzler et al., 2009); systemic exposure to CPD-0801 was higher than that to furamidine in mice given the same dose of respective prodrugs (Wu et al., 2007). These encouraging observations warrant further evaluation of CPD-0868 as an orally active agent for second-stage HAT.

Both furamidine and CPD-0801 are formed in the liver via sequential oxidative O-demethylation and reductive N-dehydroxylation reactions, producing four intermediate phase I metabolites (Fig. 1) (Zhou et al., 2004; Generaux, 2010). Once formed, active metabolites must be excreted from hepatocytes into the systemic circulation to exert antiparasitic activity. These observations led to the hypothesis that improved efficacy of the prodrug CPD-0868 against second-stage infection compared with pafuramidine reflects superior hepatobiliary disposition characteristics, including a greater extent of conversion to the active metabolite (CPD-0801) and/or more efficient efflux of CPD-0801 from hepatocytes into the systemic circulation. This hypothesis was addressed using IPLs and SCH from rats, coupled with mathematical modeling, to elucidate mechanisms underlying the difference in systemic/hepatobiliary exposure of these two antiparasitic active metabolites. Results generated from SCH were compared with IPLs.

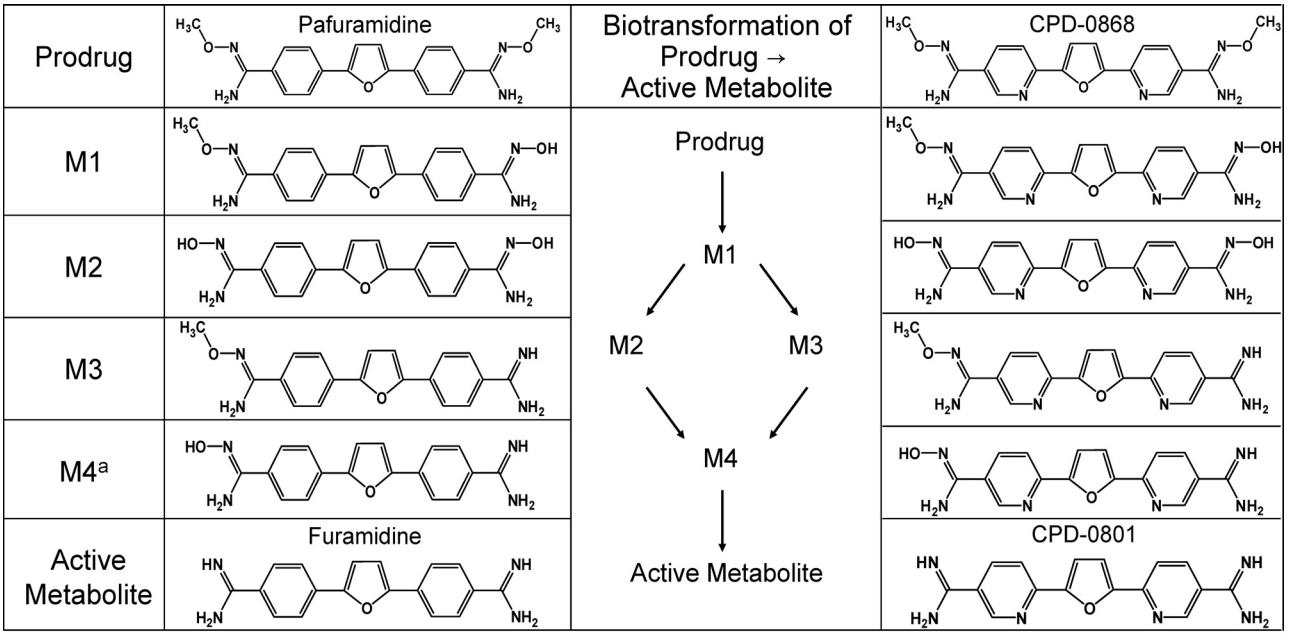

[a]*Due to lack of chemical stability, pure synthesized standards of M4 for pafuramidine and CPD-0868 were not available.*

Fig. 1. Biotransformation of prodrug to active metabolite and corresponding chemical structures.

Materials and Methods

Materials and Chemicals

Dulbecco's modified Eagle's medium (DMEM) and insulin were purchased from Invitrogen (Carlsbad, CA). ITS$^+$ (insulin/transferring/selenium) culture supplement and Matrigel were purchased from BD Biosciences Discovery Labware (Bedford, MA). Penicillin, streptomycin, fetal bovine serum, nonessential amino acids (NEAA), dexamethasone (DEX), Krebs-Henseleit buffer, Triton X-100, and taurocholate were purchased from Sigma-Aldrich (St. Louis, MO). The prodrugs pafuramidine and CPD-0868, the intermediate phase I metabolites (M1, M2, and M3) of pafuramidine, and CPD-0868, the active metabolites furamidine and CPD-0801, and the internal standards (deuterium-labeled pafuramidine, CPD-0868, furamidine, and CPD-0801) were synthesized in the laboratory of Dr. David W. Boykin (Georgia State University, Atlanta, GA) (Boykin et al., 1996; Ismail et al., 2003; Ismail and Boykin, 2006). All other chemicals and reagents were of analytical grade and used without further purification.

Animals

Male Wistar rats (250–300 g) were purchased from Charles River Laboratories (Raleigh, NC) for liver perfusion and hepatocyte isolation. Animals had free access to water and food before surgery. All animal procedures were compliant with the guidelines of the University of North Carolina Institutional Animal Care and Use Committee.

Disposition of Prodrugs/Metabolites in Isolated Perfused Rat Livers

Recirculating IPLs from rats were prepared using standard techniques; perfusions were conducted ex situ over designated times (up to 2 h) in a temperature-controlled chamber with recirculating oxygenated Krebs-Henseleit buffer (80 ml) containing 20% (v/v) rat blood at a flow rate of 20 ml/min (Brouwer and Thurman, 1996). Taurocholate was infused (30 μmol/h) into the perfusate reservoir to maintain bile flow. Prodrug (pafuramidine or CPD-0868) stock solution (80 μl; 10 mM in DMSO) was added as a bolus to the perfusate reservoir to yield an initial concentration of 10 μM (0.1% DMSO). Aliquots of perfusate (~400 μl) were collected from the IPL reservoir at 5-min intervals from 0 to 40 min and at 10-min intervals thereafter up to 2 h during perfusion; bile was collected at 10-min intervals; liver was harvested at the end of perfusion. Perfusate plasma, bile, and liver collections were stored at −80°C pending analysis for prodrug and derived metabolites by liquid chromatography with detection by tandem mass spectrometry (LC-MS/MS). The prodrug concentration (10 μM) was based on solubility in perfusate and assay sensitivity to monitor prodrugs/metabolites in perfusate, liver, and bile throughout the 2-h experimental period. The absence-of-liver condition was used to assess nonspecific binding of prodrug and metabolites to the IPL apparatus.

Determination of Unbound Fraction

Liver. Livers from IPL experiments (described above) were thawed and homogenized in three volumes (v/w) of 0.1 M phosphate-buffered saline (PBS). The unbound fraction of formed active metabolite in liver homogenates was determined using rapid equilibrium dialysis devices (Thermo Fisher Scientific, Waltham, MA). Liver homogenates (200 μl) and blank PBS (350 μl) were placed in tissue and buffer chambers, respectively, and incubated (37°C) for 6 h on a thermomixer (350 rpm) (Eppendorf AG, Hamburg, Germany). Preliminary testing indicated that 6 h of incubation was sufficient to achieve equilibrium without significant compound degradation. After 6 h, aliquots (100 μl) were collected from the tissue and buffer chambers and analyzed for total (bound + unbound) and unbound formed active metabolite, respectively, by LC-MS/MS.

Perfusate/Plasma. Blank rat IPL perfusate (composed of 20% rat blood) and plasma were spiked with preformed active metabolite to yield a total concentration of 1 or 10 μM. Spiked perfusate/plasma (200 μl) and blank PBS (350 μl) were placed in corresponding dialysis chambers, incubated for 6 h, and analyzed for total (bound + unbound) and unbound preformed active metabolite, respectively, by LC-MS/MS.

Disposition of Prodrugs/Metabolites in Sandwich-Cultured Rat Hepatocytes

Freshly isolated rat hepatocytes were seeded at 1.75×10^6 cells/well onto six-well BioCoat collagen plates (BD Biosciences Discovery Labware) in seeding medium [DMEM containing 5% (v/v) fetal bovine serum, 10 μM insulin, 1 μM DEX, 2 mM L-glutamine, 1% (v/v) NEAA, 100 units penicillin G sodium, and 100 μg of streptomycin sulfate]. Approximately 24 h after seeding (day 1), cells were overlaid with 0.25 mg/ml Matrigel in ice-cold culture medium [DMEM supplemented with 1% (v/v) ITS$^+$ (insulin/transferrin/selenium), 1 μM DEX, 2 mM L-glutamine, 1% (v/v) NEAA, 100 units penicillin G sodium, and 100 μg/ml streptomycin sulfate]. Thereafter, culture medium was changed every 24 h for 2 days. On day 4, cells were incubated with culture medium (1.5 ml) containing pafuramidine or CPD-0868 at a concentration identical to that used for the IPL experiments (10 μM, 0.1% DMSO). At designated times up to 24 h, aliquots of medium (500 μl) were collected, and cells were washed twice and incubated at 37°C for 5 min with Hanks' balanced salt solution (HBSS) with Ca^{2+} (to maintain bile canalicular networks; cells + bile) or without Ca^{2+} (to open bile canalicular spaces; cells) (Lee et al., 2010). After incubation, buffer was removed, and cells were lysed with ice-cold methanol/water [7:1 (v/v)] containing 0.1% (v/v) trifluoroacetic acid. Media, cell lysates, and cells + bile lysates were stored at −80°C pending analysis for prodrug and derived metabolites by LC-MS/MS. The absence-of-cell condition was used to assess nonspecific binding of prodrug and metabolites to Matrigel-overlaid BioCoat collagen plates.

Determination of Hepatocyte Viability

Effect of prodrugs/metabolites on hepatocyte viability was assessed by monitoring lactate dehydrogenase (LDH) release to the culture medium using a cytotoxicity detection kit (Roche Diagnostics, Indianapolis, IN) according to the manufacturer's instructions. In brief, aliquots (25 μl) of medium from vehicle-treated (0.1% DMSO) and prodrug-treated SCH were collected at 0.5, 2, 4, 8, and 24 h. The degree of LDH release was expressed as the percentage of the maximum cellular LDH release, which was measured by adding 2% detergent, Triton X-100, to SCH (Lee et al., 2008).

LC-MS/MS Analysis for Prodrugs and Derived Metabolites

The concentration of prodrug and derived metabolites in perfusate/plasma or medium, liver homogenates or cell lysates, bile, and PBS from IPL or SCH studies (described above) was quantified by LC-MS/MS using a method modified from Wang et al. (2006). In brief, analytes were extracted by adding methanol/H_2O (7:1) with 0.1% trifluoroacetic acid containing 600 nM internal standards, followed by vigorous mixing and centrifugation at 1800*g* for 10 min. The supernatant (100 μl) was transferred to HPLC vials and quantified for prodrug and metabolite using multiple reaction monitoring via an API 4000 triple quadrupole mass spectrometer (Applied Biosystems, Foster City, CA) equipped with a Turbo IonSpray interface (Applied Biosystems/MDS Sciex, Foster City, CA). Analytes were separated on an Aquasil C18 HPLC column (2.1 mm × 50 mm, 5 μm) (Thermo Fisher Scientific) with a high-pressure linear gradient program consisting of 0.1% formic acid in HPLC-grade water (A) and 0.1% formic acid in HPLC-grade methanol (B) delivered by a Shimadzu pumping system (Shimadzu, Kyoto, Japan) at a flow rate of 0.75 ml/min as follows: after a 0.5-min initial hold at 10% B, mobile phase composition was increased from 10 to 90% B over 3.5 min and

held at 90% B for 0.5 min; the column was re-equilibrated for 0.5 min before the next injection. For all studies except liver binding, prodrugs and metabolites were quantified with calibration standards (1–10,000 nM) prepared in the appropriate matrix; for the liver binding study, both active metabolites were quantified with calibration standards prepared in liver homogenates (0.5–50 μM) and PBS (1–10,000 nM). All calibration curves were linear over the respective range ($R^2 > 0.98$). Intraday and interday coefficients of variation were <15%.

Pharmacokinetic Modeling

Stepwise nonlinear least-squares regression analysis (WinNonlin 5.0.1; Pharsight, Mountain View, CA) was used to fit a compartmental model (Fig. 2, model 1) to the hepatobiliary disposition of prodrug and derived metabolites mass versus time data obtained from IPLs and SCH. Model 2 (Fig. 2) incorporates the unbound fraction of active metabolite in the liver to emphasize the importance of hepatic binding in governing the systemic exposure of these compounds. Goodness of fit was based on randomness of residuals, correlation matrices, standard errors of parameter estimates, and visual comparison of predicted mass/concentration-time profiles with observed data. Because the batch of synthesized pafuramidine standard contained impurities largely as the intermediate metabolite, M3, an initial value of 10% of pafuramidine in the dosing compartment (perfusate for IPLs; medium for SCH) was used to describe M3 disposition in IPLs and SCH. Some intermediate metabolites (specifically, M1 and M2 of pafuramidine and M2 of CPD-0868) were not included in the model if concentrations in the perfusate/medium, liver/cells, and bile were below the limit of quantification (BLQ) or if pure synthesized standards (M4 of pafuramidine and CPD-0868) were not available.

Data Analysis

The hepatic clearance (milliliters per minute) and extraction ratio of prodrug in IPLs were calculated as follows.

Total hepatic clearance (Cl_H) = dose/$AUC_{perfusate,0-\infty}$, where $AUC_{perfusate,0-\infty}$ was calculated as the area under the perfusate concentration-time curve from time 0 to infinity using the trapezoidal method.

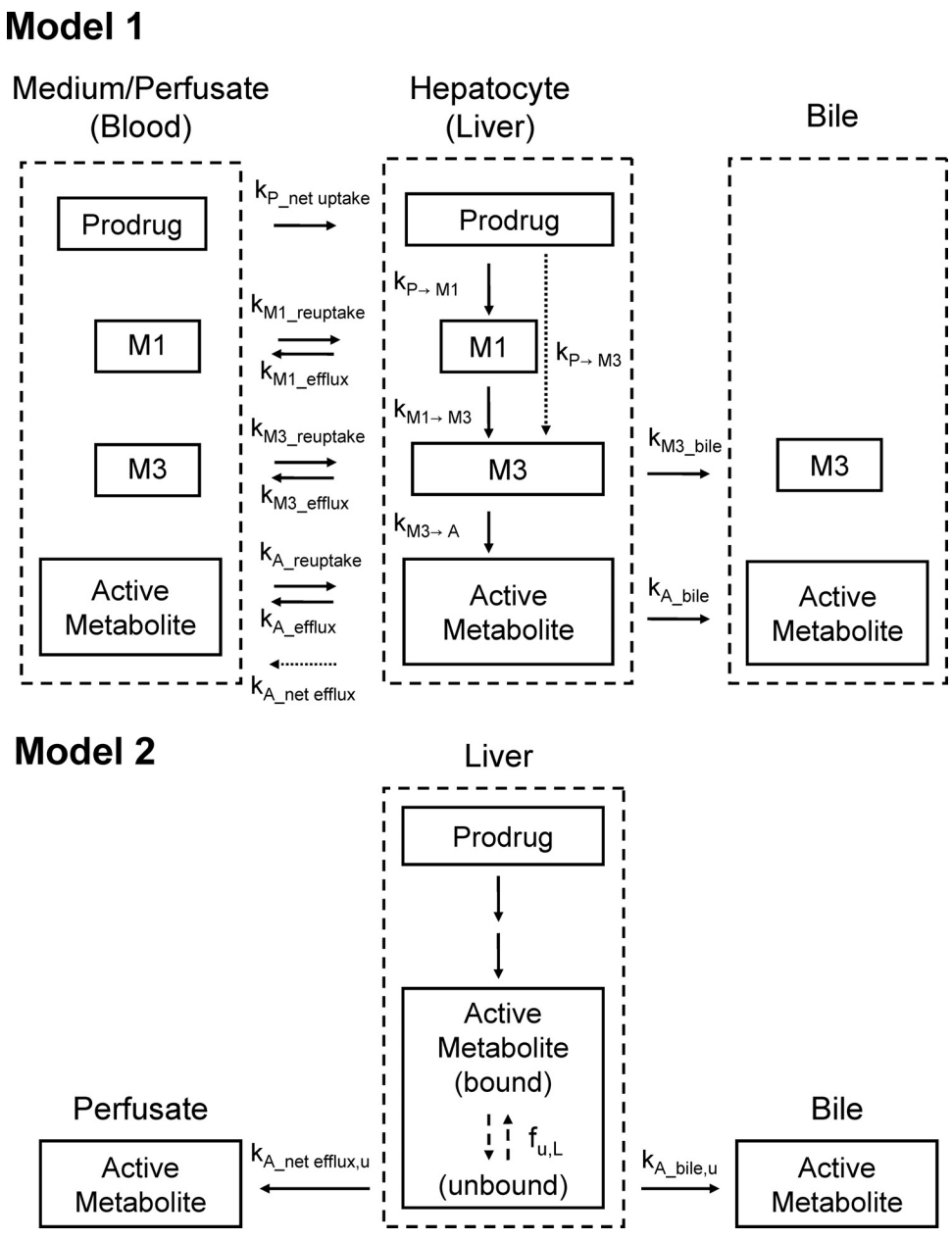

Fig. 2. Model schemes depicting disposition of prodrugs/metabolites in rat IPLs and SCH (model 1) and hepatic excretion of unbound active metabolite in rat IPLs (model 2). $k_{P\_net\ uptake}$, the first-order rate constant for net hepatic uptake of prodrug; $k_{P\rightarrow M1}$, the first-order rate constant for metabolic conversion from prodrug to intermediate metabolite M1; k_{M1_efflux} and $k_{M1\_reuptake}$, the first-order rate constants for hepatic basolateral efflux and reuptake of M1, respectively; $k_{P\rightarrow M3}$, the first-order rate constant for metabolic conversion from prodrug (pafuramidine only) to intermediate metabolite M3; $k_{M1\rightarrow M3}$, the first-order rate constant for metabolic conversion from M1 to M3; k_{M3_efflux}, $k_{M3\_reuptake}$, and k_{M3_bile}, the first-order rate constants for hepatic basolateral efflux, reuptake, and biliary excretion of M3, respectively; $k_{M3\rightarrow A}$, the first-order rate constant for metabolic conversion from M3 to active metabolite; k_{A_efflux}, $k_{A\_reuptake}$, $k_{A\_net\ efflux}$, and k_{A_bile} the first-order rate constants for hepatic basolateral efflux, reuptake, net basolateral efflux, and biliary excretion of active metabolite, respectively; $f_{u,L}$, hepatic unbound fraction of active metabolite; $k_{A\_net\ efflux,u}$ and $k_{A\_bile,u}$, first-order rate constants for hepatic basolateral net efflux and biliary excretion of unbound active metabolite, respectively.

Biliary clearance (Cl_b) = $mass_{bile,0-120min}/AUC_{perfusate,0-120min}$, where $mass_{bile,0-120min}$ was calculated as the cumulative amount of compound excreted into bile over 120 min.

Metabolic clearance (Cl_m) = $Cl_H - Cl_b$.

Hepatic extraction ratio (E_H) = Cl_H/Q, where Q represents total perfusate flow rate (20 ml/min). [The blood-to-plasma ratio for both prodrugs is 1 (unpublished observations).]

With both IPLs and SCH, hepatic accumulation was calculated as the amount of active metabolite recovered in the liver or cells as a percentage of the total amount formed over time. Extent of formation of active metabolite was determined as the total amount of active metabolite recovered in perfusate, liver, and bile as a percentage of the initial amount of prodrug added to the perfusate reservoir (IPLs) or the total amount of active metabolite recovered in medium, cells, and bile as a percentage of the initial amount of prodrug added to the culture medium (SCH).

Data showed that distribution of furamidine/CPD-0801 between liver and perfusate in IPLs, and between cells and medium in SCH, reached equilibrium from 100 min and 16 h onward, respectively. Therefore, furamidine/CPD-0801 liver-to-perfusate (IPLs) or cell-to-medium (SCH) partition coefficients ($K_{p,IPLs}$ and $K_{p,SCH}$, respectively) were calculated as the ratio of concentration in liver (C_L) to that in perfusate (C_{Per}) at the end of the perfusion (120 min) or the ratio of concentration in cells (C_C) to that in medium (C_M) at the end of the incubation (24 h). The hepatocellular volumes used to calculate C_L and C_C were 0.6 ml/g rat liver (Pang et al., 1988) and 6.2×10^{-6} μl/hepatocyte (Swift et al., 2010) for IPLs and SCH, respectively.

A two-tailed Student's t test was used to compare disposition properties between furamidine and CPD-0801 in IPLs and SCH. A p value <0.05 was considered statistically significant.

Results

Nonspecific Binding of Prodrugs/Metabolites. Nonspecific binding of both prodrugs and all metabolites to collagen-coated culture plates, and to the perfusion tubing and apparatus, was <10% of the initial mass of starting material. Accordingly, nonspecific binding was assumed to be negligible.

Disposition of Prodrugs/Metabolites in Isolated Perfused Rat Livers. Both prodrugs were taken up and metabolized rapidly, as reflected by the prompt appearance of intermediate metabolites in perfusate (Fig. 3). Both prodrugs were eliminated in rat liver primarily by metabolism; biliary excretion was negligible (Table 1). Pafuramidine had a higher hepatic extraction ratio than CPD-0868 (Table 1). Recovery of M1 and M2 metabolites of pafuramidine in perfusate, liver, and bile was BLQ. The M3 metabolite of pafuramidine appeared in the perfusate immediately (Fig. 3A), reflecting M3 as an impurity in this batch of synthesized standard of pafuramidine, and then decreased slightly because of uptake into hepatocytes; at ~10 min, M3 began to increase slightly because of the efflux of M3 formed from M1. The M1 metabolite of CPD-0868 in perfusate was maximal at ~15 min (Fig. 3B), then decreased rapidly, because of reuptake into hepatocytes and further metabolism. The M3 metabolite of CPD-0868 in perfusate was maximal at ~40 min (Fig. 3B), then decreased because of reuptake into hepatocytes and further metabolism. The rate constants associated with both basolateral reuptake ($k_{M3\_reuptake}$) and efflux (k_{M3_efflux}) of the M3 metabolite were comparable between prodrugs (Table 2). $k_{M3\_reuptake}$ was more than 40-fold higher than k_{M3_efflux} for the M3 metabolite of both prodrugs (Table 2). The rate constant associated with biliary excretion of the M3 metabolite (k_{M3_bile}) of CPD-0868 was 4-fold higher than that of the M3 metabolite of pafuramidine (Table 2). The rate constant associated with conversion from M3 to the active metabolite ($k_{M3\rightarrow A}$) of CPD-0868 was 3.5-fold higher than that of pafuramidine (Table 2).

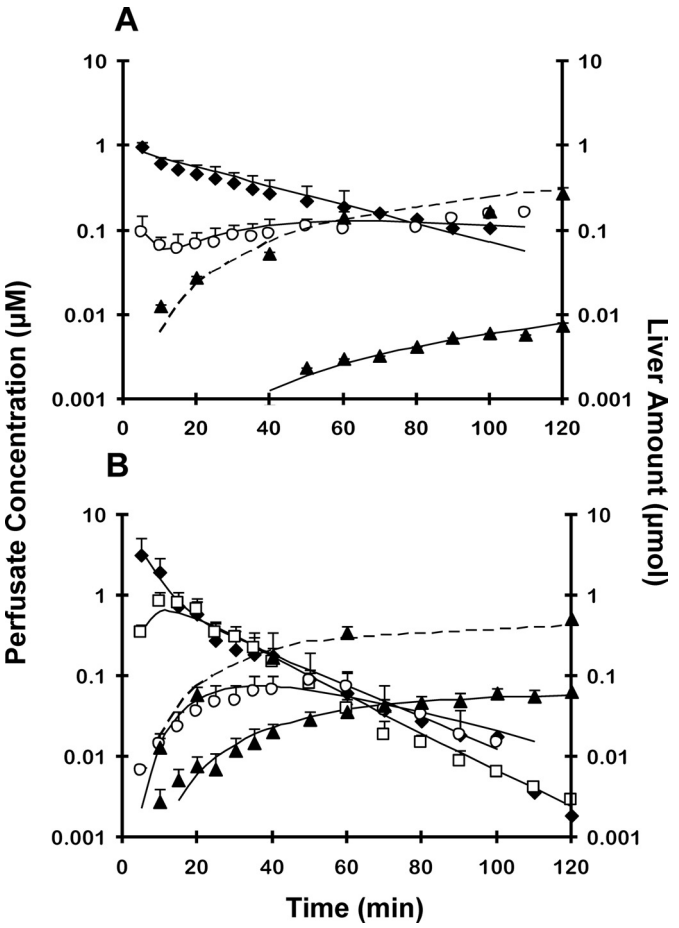

Fig. 3. Disposition of prodrugs pafuramidine (A) and CPD-0868 (B), and corresponding metabolites over 120 min in rat isolated perfused livers. Prodrug (10 μM) was administered as a bolus to the perfusion reservoir, which contained 80 ml of 20% (v/v) rat blood. ♦, prodrug; □, M1; ○, M3; ▲, active metabolite. Symbols and error bars for perfusate concentrations denote means and SDs, respectively, of $n = 5$ livers. Symbols and error bars for liver mass denote means and SDs, respectively, of $n = 5$ livers, using a destructive sampling strategy. Solid lines represent perfusate concentration-time profile of prodrug and derived metabolites. Dashed lines represent liver amount-time profile of active metabolite. Solid and dashed lines represent the computer-generated best fit of the pharmacokinetic scheme depicted in Fig. 2 (model 1) to the data. Note: pafuramidine contained 5 to 10% impurities, largely as M3; M1 from pafuramidine is not included in A because of low recovery in perfusate, as described under *Results*.

TABLE 1
Hepatic clearance and extraction ratio of prodrugs in rat isolated perfused livers

Prodrug	Hepatic Clearance			E_H
	Total	Metabolic	Biliary	
	ml/min			
Pafuramidine	17.6	17.6	<0.1	0.88
CPD-0868	12.4	12.4	<0.1	0.62

The extent of formation of furamidine in rat IPLs was at least half that of CPD-0801 (Fig. 4A). Perfusate exposure to CPD-0801 was much higher compared with furamidine. The AUC for CPD-0801 was 10-fold higher than that for furami-

TABLE 2

Kinetic parameters, generated from model 1, associated with the disposition of prodrugs (pafuramidine and CPD-0868) and derived metabolites in rat isolated perfused livers

Kinetic parameters are defined in the legend to Fig. 2. No discernable correlation between parameters was observed by evaluation of the correlation matrix (absolute correlation value ≤0.5). See Supplemental Fig. S1 for the plot of weighted residual vs. time data.

Parameter	Pafuramidine/Metabolites		CPD-0868 / Metabolites	
	Estimate	CV	Estimate	CV
	h^{-1}	%	h^{-1}	%
$k_{P\_net\ uptake}$	58	88	13	23
$k_{P\rightarrow M1}$	N.A.[b]	N.A.	3.8	7
$k_{M1\_reuptake}$	N.A.	N.A.	96	55
k_{M1_efflux}	N.A.	N.A.	330	62
$k_{P\rightarrow M3}$	1.7	6	N.A.	N.A.
$k_{M1\rightarrow M3}$	N.A.	N.A.	108	20
$k_{M3\_reuptake}$	13	69	11	33
k_{M3_efflux}	0.31	72	0.20	29
k_{M3_bile}	0.096	11	0.42	14
$k_{M3\rightarrow A}$	0.43	8	1.5	12
$k_{A\_reuptake}$	2.7	>100	3.3	>100
k_{A_efflux}	0.0065	>100	0.028	>100
$k_{A\_net\ efflux}$[a]	0.0021	14	0.012	51
k_{A_bile}	0.020	48	0.0084	61

N.A., not applicable.

[a] Because of the high variability associated with the parameter estimates for $k_{A,reuptake}$ and k_{A_efflux}, model 1 was modified to include a net efflux term, $k_{A\_net\ efflux}$.

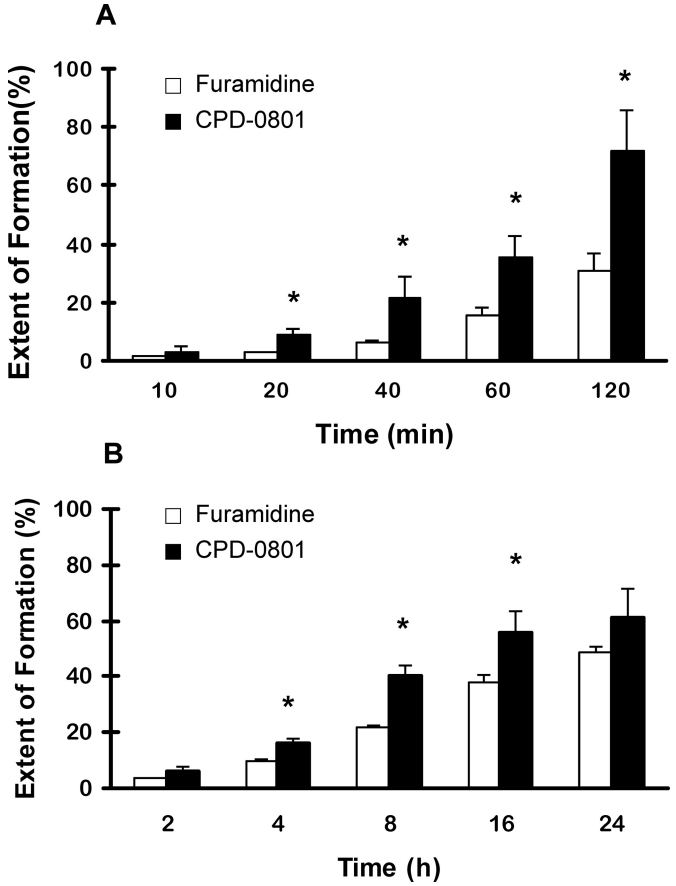

Fig. 4. Extent of formation of active metabolites represented as total amount of active metabolite recovered in perfusate, liver, and bile as a percentage of the initial amount of prodrug added to the perfusate reservoir from isolated perfused rat liver experiments (A; mean ± S.D., n = 5 livers) and total amount of active metabolite recovered in medium, cells, and bile as a percentage of the initial amount of prodrug added to the culture medium from sandwich-cultured rat hepatocyte experiments (B; mean ± S.D., n = 2 livers in duplicate). *, $p < 0.05$ versus furamidine (two-tailed Student's t test).

dine (Table 3). Pharmacokinetic modeling (Fig. 2, model 1) revealed that the rate constant associated with net basolateral efflux ($k_{A\_net\ efflux}$) of CPD-0801 was 6-fold higher than that of furamidine (Table 2).

Hepatic accumulation of both active metabolites in rat IPLs was extensive (Table 3). The liver-to-perfusate partition coefficient ($K_{p,IPLs}$) of furamidine at 2 h was 3700 and was approximately 5-fold higher than that of CPD-0801 (Table 3). The unbound fractions of both active metabolites in plasma/perfusate were similar at 1 and 10 μM. The unbound fraction of each active metabolite in rat liver ($f_{u,L}$) was ≥24-fold lower than that in plasma ($f_{u,P}$) and perfusate (composed of 20% rat blood; $f_{u,Per}$) (Table 3). The $f_{u,L}$ of CPD-0801 was approximately 5-fold higher than that of furamidine (Table 3). Assuming that only unbound drug can translocate out of hepatocytes into blood and bile, $f_{u,L}$ was incorporated into the pharmacokinetic model (Fig. 2, model 2) to evaluate further the hepatic excretion of derived active metabolite. Based on model 2, the rate constant for biliary excretion ($k_{A\_bile,u}$) was 9-fold higher than that of basolateral efflux ($k_{A\_net\ efflux,u}$) for unbound furamidine, whereas $k_{A\_bile,u}$ and $k_{A\_net\ efflux,u}$ for CPD-0801 were more comparable than those for furamidine (Table 4). After incorporating $f_{u,L}$, the $k_{A\_net\ efflux,u}$ of furamidine became comparable with that of CPD-0801 (Table 4).

Disposition of Prodrugs/Metabolites in Day-4 Sandwich-Cultured Rat Hepatocytes. The disposition profiles of prodrugs and derived metabolites in SCH (Fig. 5) were similar to those for rat IPLs (Fig. 3), although the time course in SCH was longer than that in IPLs (24 versus 2 h). As shown in IPLs, the recovery of M1 and M2 metabolites of pafuramidine in medium, cells, and bile was BLQ; the M3 metabolite of pafuramidine appeared in medium immediately (Fig. 5A), reflecting M3 as an impurity. The M1 metabolite of CPD-0868 in medium was maximal at 2 h (Fig. 5B), and then decreased rapidly because of subsequent reuptake into hepatocytes and metabolism. The M3 metabolite of CPD-0868 in medium was maximal at 8 h (Fig. 5B), then decreased because of reuptake into hepatocytes and further metabolism. The rate constant associated with conversion from M3 to the active metabolite ($k_{M3\rightarrow A}$) of CPD-0868 was 1.4-fold higher than that of pafuramidine (Table 5). Only the M3 metabolite of CPD-0868 was recovered in bile (Table 5).

The extent of conversion of CPD-0868 to CPD-0801 was consistently higher than that of pafuramidine to furamidine in SCH over 24 h (Fig. 4B). Medium exposure to CPD-0801 was higher compared with furamidine. The AUC for CPD-0801 was 7-fold higher than that for furamidine (Table 3). As shown in IPLs, $k_{A\_net\ efflux}$ of CPD-0801 was 6-fold greater than that of furamidine. Model 1 adequately described the disposition of furamidine in medium and hepatocytes (solid and dashed lines in Fig. 5A); the large variability in the parameter estimate for $k_{A\_net\ efflux}$ of furamidine may be caused by the marked difference between the amount of furamidine recovered in the medium and that recovered in hepatocytes (>two orders of magnitude). Hepatocellular accumulation of furamidine and CPD-0801 over 24 h was extensive (Table 3). The cell-to-medium partition coefficients of both active metabolites measured in SCH ($K_{p,SCH}$) was 6- to 7-fold higher than liver-to-perfusate partition coefficients measured in IPLs ($K_{p,IPLs}$); similar to IPL results, $K_{p,SCH}$ of furamidine was 5- to 6-fold higher than that of CPD-0801 (Table 3).

TABLE 3

Comparison of hepatic disposition of active metabolites in IPLs and day-4 SCH from rats

Comparisons between furamidine and CPD-0801 for all outcomes were made using the two-tailed Student's *t* test (* $p < 0.05$ vs. furamidine). Values denote mean ± S.D.

Outcome	Rat IPLs		Rat SCH	
	Furamidine	CPD-0801	Furamidine	CPD-0801
Hepatic accumulation (%)	99 ± 1	97 ± 1	99 ± 0	95 ± 1*
Extent of formation (%)[a]	31 ± 6	72 ± 14*	49 ± 2	61 ± 11
Perfusate or medium AUC (μM·h)[b]	0.006 ± 0.002	0.06 ± 0.01*	0.6 ± 0.1	4.2 ± 0.3*
Liver-to-perfusate or cell-to-medium partition coefficient	3700	800	27,000	4700
$f_{u,L}$ (%)[c]	0.3 ± 0.1	1.6 ± 0.3*	N.A.	N.A.
$f_{u,Per}$ (%)[d]	44 ± 5	70 ± 6*	N.A.	N.A.
$f_{u,P}$ (%)[d]	24 ± 2	38 ± 3*	N.A.	N.A.

N.A., not applicable.
[a] Measured at the end of the perfusion for IPLs (120 min) and at the end of the incubation for SCH (24 h).
[b] Calculated as the AUC from 0 to 2 h (IPL) and from 0 to 24 h (SCH), respectively.
[c] Unbound fraction of formed active metabolite in liver.
[d] Unbound fraction of preformed active metabolite added to perfusate or plasma at 1 μM.

TABLE 4

Kinetic parameters, generated from model 2, associated with the hepatic excretion of unbound active metabolites in rat isolated perfused livers

Kinetic parameters are defined in the legend to Fig. 2.

Unbound Active Metabolite	$k_{A\_net\ efflux,u}$		$k_{A\_bile,u}$	
	Estimate	CV	Estimate	CV
	h^{-1}	%	h^{-1}	%
Furamidine	0.66	16	6.0	19
CPD-0801	0.60	42	0.74	40

Effect of Prodrugs/Metabolites on Hepatocyte Viability. In rat SCH treated with vehicle (0.1% DMSO) or prodrug (pafuramidine or CPD-0868), an elevation in LDH release was not observed over 24 h compared with untreated SCH (data not shown). These data suggested that membrane integrity remained intact as a function of prodrug treatment and time.

Discussion

SCH have been used previously to investigate the hepatobiliary disposition of drug/metabolite pairs, including terfenadine and fexofenadine (Turncliff et al., 2006). The current work represents the first systematic comparison of two established hepatic models, IPLs and SCH, to understand mechanisms governing the systemic and hepatobiliary exposure of two antiparasitic active metabolites. Rat IPLs and SCH showed similar disposition profiles of prodrugs and derived metabolites (Fig. 3 versus Fig. 5). The extent of formation and AUC in perfusate (IPLs) or medium (SCH) of CPD-0801 was consistently higher than that of furamidine (Table 3). A stepwise pharmacokinetic modeling approach was used to differentiate, quantitatively, between the contribution of hepatic metabolism and transport to the enhanced perfusate/medium AUC of CPD-0801 compared with furamidine. Model 1 described adequately the disposition of both prodrugs and derived metabolites (Figs. 3 and 5; Supplemental Figs. S1 and S2) and predicted a net basolateral efflux rate constant ($k_{A\_net\ efflux}$) for CPD-0801 that was 6-fold higher than that for furamidine in both IPLs (Table 2) and SCH (Table 5). The extent of formation of CPD-0801 was only ≤2.5-fold higher than that of furamidine (Fig. 4; Table 3).

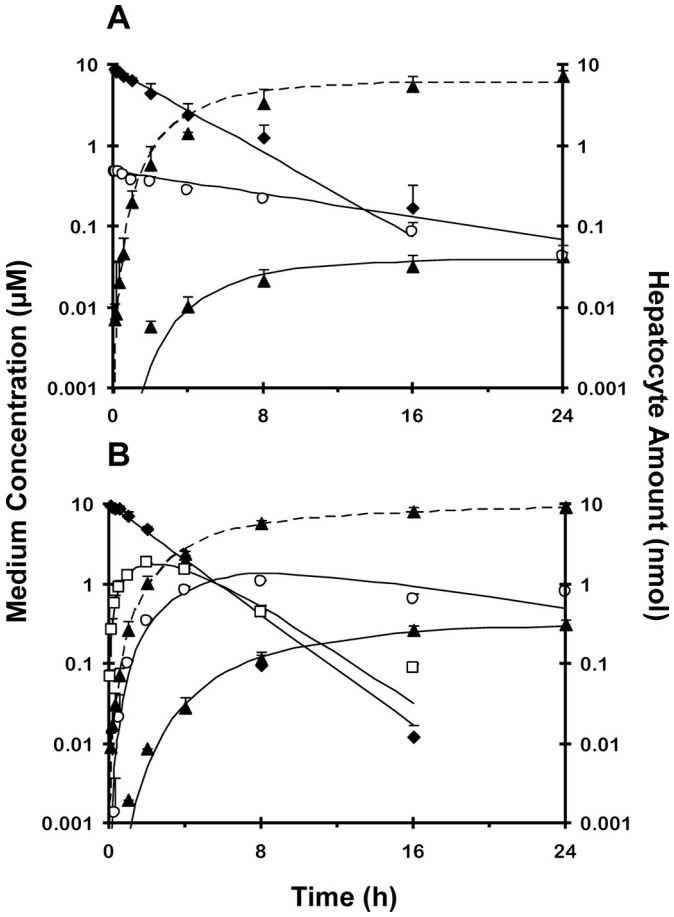

Fig. 5. Disposition of prodrugs pafuramidine (A) and CPD-0868 (B) and corresponding metabolites over 24 h in day-4 sandwich-cultured rat hepatocytes. Prodrug (10 μM) was administered as a bolus to each well, which contained 1.5 ml of culture medium. ♦, prodrug; □, M1; ○, M3; ▲, active metabolite. Symbols and error bars denote means and SDs, respectively, of $n = 2$ livers in duplicate. Solid lines represent medium concentration-time profile of prodrug and derived metabolites. Dashed lines represent hepatocyte amount-time profile of active metabolite. Solid and dashed lines represent the computer-generated best fit of the pharmacokinetic model depicted in Fig. 2 (model 1) to the data. Pafuramidine contained 5 to 10% impurities, primarily M3; M1 from pafuramidine is not included in A because of low recovery in medium, as described under *Results*.

TABLE 5

Kinetic parameters, generated from model 1, associated with disposition of prodrugs (pafuramidine and CPD-0868) and derived metabolites in day-4 rat SCH

Kinetic parameters are defined in the legend to Fig. 2. No discernable correlation between parameters was observed by evaluation of the correlation matrix (absolute correlation value ≤0.5). See Supplemental Fig. S2 for the plot of weighted residual vs. time data.

Parameter	Pafuramidine/Metabolites		CPD-0868/Metabolites	
	Estimate	CV	Estimate	CV
	h^{-1}	%	h^{-1}	%
$k_{P\_net\ uptake}$	0.30	7	0.40	4
$k_{P\rightarrow M1}$	N.A.[b]	N.A.	67	37
$k_{M1\_reuptake}$	N.A.	N.A.	3.5	29
k_{M1_efflux}	N.A.	N.A.	71	42
$k_{P\rightarrow M3}$	1.3	26	N.A.	N.A.
$k_{M1\rightarrow M3}$	N.A.	N.A.	12	40
$k_{M3\_reuptake}$	0.080	90	0.15	30
k_{M3_efflux}	N.A.	N.A.	0.35	27
k_{M3_bile}	N.A.	N.A.	0.050	55
$k_{M3\rightarrow A}$	0.46	16	0.66	15
$k_{A\_reuptake}$	0.83	>100	0.27	>100
k_{A_efflux}	0.0080	>100	0.015	>100
$k_{A\_net\ efflux}$[a]	0.00076	>100	0.0046	27
k_{A_bile}	N.A.	N.A.	N.A.	N.A.

N.A., not applicable.

[a]Because of the high variability associated with the parameter estimates for $k_{A,reuptake}$ and k_{A_efflux}, model 1 was modified to include a net efflux term, $k_{A\_net\ efflux}$.

These observations indicated that net basolateral efflux predominated over metabolism in governing perfusate/medium exposure to active metabolite.

The $f_{u,L}$ of CPD-0801 was ~5-fold higher than that of furamidine. Based on model 2 (Fig. 2), the ratio of biliary excretion ($k_{A\_bile,u}$) to basolateral efflux ($k_{A\_net\ efflux,u}$) rate constants for furamidine was 9 (Table 4), suggesting that once formed in liver, the predominant process that determines furamidine elimination is excretion into bile, whereas biliary and basolateral excretory processes contribute approximately equally to CPD-0801 hepatic excretion (Table 4). Incorporation of $f_{u,L}$ in model 2 (Fig. 2) resulted in a comparable $k_{A\_net\ efflux,u}$ of both active metabolites (Table 4), indicating that the 6-fold difference in the rate constant for net basolateral efflux of total formed active metabolite ($k_{A\_net\ efflux}$) could be attributed largely to the 5-fold difference in hepatic binding.

During an expanded phase I safety study in indigenous African volunteers, pafuramidine demonstrated transiently elevated liver transaminanses, a known class effect of diamidines (Paine et al., 2010). In rats administered a single oral dose of pafuramidine (10 mg/kg), liver-to-plasma partitioning (K_p) of furamidine was as high as 1300 (Midgley et al., 2007). As shown in the current study, hepatic accumulation of furamidine was extensive, and the unbound fraction of furamidine in liver was at least 80-fold lower than that in plasma and perfusate (Table 3). Thus, binding sites in liver may act as an "intracellular sink" that limit systemic exposure to furamidine. Previous subcellular fractionation studies demonstrated that furamidine accumulated primarily in the mitochondrial fraction of liver tissue (Midgley et al., 2007). Consistent with these observations, preliminary fractionation studies with rat IPLs revealed that furamidine was localized primarily in the mitochondrial fraction (43%); CPD-0801 was localized primarily in the cytosolic fraction (45%), with negligible mitochondrial accumulation (≤1%) (unpublished observations). Extensive accumulation of furamidine in mitochondria could cause mitochondrial dysfunction and trigger liver signal elevations (Pessayre et al., 1999). Significant hepatic accumulation of furamidine is consistent with previous in vivo data (Midgley et al., 2007), suggesting that hepatocellular sequestration may limit systemic exposure of furamidine and predispose the liver to elevated signals. In contrast, a significantly higher hepatic unbound fraction and less mitochondrial accumulation of CPD-0801, compared with furamidine, could enhance systemic exposure to CPD-0801 and reduce hepatic signals.

Using appropriate preclinical hepatic models to estimate liver-to-plasma partitioning of potential hepatotoxicants has been a topic of interest in toxicologic risk assessment. In the current study, the liver-to-perfusate partition coefficient ($K_{p,IPLs}$) of furamidine measured in IPLs was 3700, approximately 2.8-fold higher than the in vivo K_p (1300) measured in rats. This discrepancy can be explained by the 2-fold difference in the extent of protein binding of furamidine in perfusate (composed of 20% blood) versus plasma (Table 3). If basolateral membrane barriers are absent, liver-to-plasma partitioning can be estimated as the ratio of the unbound fraction of furamidine in plasma to that in liver (i.e., $K_p = f_{u,P}/f_{u,L} = 24/0.3 = 80$), assuming the liver is a well stirred organ (Rowland, 1985). Likewise, $K_{p,IPLs} = f_{u,Per}/f_{u,L} = 44/0.3 = 147$. Both estimated K_p and $K_{p,IPLs}$ values are much lower than observed values in IPLs and intact rats, suggesting that active transport may be involved in the increased hepatic partitioning of furamidine in the intact organ. It is noteworthy that cell-to-medium partition coefficients of furamidine/CPD-0801 measured in SCH ($K_{p,SCH}$) overestimated corresponding values measured in IPLs ($K_{p,IPLs}$) by approximately 6-fold. This discrepancy could be explained, in part, by the absence of serum in culture medium, which resulted in a higher f_u in medium (approximately unity) than that in perfusate. Therefore, binding differences in transport buffer/medium and plasma need to be considered when using SCH to estimate liver-to-plasma partitioning. Nonetheless, both $K_{p,SCH}$ and $K_{p,IPLs}$ of furamidine were >5-fold higher than those of CPD-0801.

The intermediate metabolite, M3, from both prodrugs was excreted extensively into bile in IPLs; M3 from CPD-0868 was the most extensively excreted compound in bile among all prodrugs and metabolites. Both active metabolites also were recovered in bile, but to a 20- to 50-fold lesser extent than M3 from CPD-0868 (Table 2). In contrast, only M3 from CPD-0868 was recovered in bile of SCH. Unlike in IPLs, biliary excretion in SCH was measured indirectly, by determining the difference in substrate accumulation between standard HBSS (cells + bile) and Ca^{2+}-free HBSS (cells) (Liu et al., 1999b). As reported previously, SCH may underpredict in vivo biliary clearance of compounds because of a less extensive canalicular network formation relative to whole liver (Liu et al., 1999b; Hoffmaster et al., 2005; Abe et al., 2008). To compare the biliary excretion in SCH and IPLs, the intrinsic biliary clearance of M3 from CPD-0868 in SCH ($Cl_{M3\_biliary,\ SCH}$) was estimated by multiplying k_{M3_bile} (Table 5) by the hepatocellular volume of 6.2×10^{-6} μl/hepatocyte (Swift et al., 2010), and then scaled up to liters per hour per gram of liver based on 110×10^6 hepatocytes/g rat liver (Ito and Houston, 2004) and 10^6 hepatocytes/well in six-well plates. The intrinsic biliary clearance of M3 from CPD-0868 in IPLs ($Cl_{M3\_biliary,\ IPLs}$) was estimated by multiplying k_{M3_bile}

(Table 2) by the hepatocellular volume of 0.6 ml/g rat liver (Pang et al., 1988). Scaled $Cl_{M3\_biliary,\ SCH}$ approximated $Cl_{M3\_biliary,\ IPLs}$ (3.4×10^{-5} versus 25×10^{-5} l/h/g liver) within an order of magnitude. As shown in rat IPLs, the fraction of total formed furamidine and CPD-0801 excreted into bile at 2 h was ≤3% (calculated by subtraction of the percentage of hepatic accumulation from unity; Table 3); in addition, k_{A_bile} of furamidine and CPD-0801 was 20- to 50-fold lower compared with M3 (k_{M3_bile}) from CPD-0868 (Table 2). Therefore, biliary excretion of furamidine/CPD-0801 may be so small that the difference in substrate accumulation between standard and Ca^{2+}-free HBSS was indistinguishable.

A previous study showed that CYP4F2 and CYP4F3B were the major enzymes responsible for pafuramidine O-demethylation (M1 formation) in human liver microsomes (Wang et al., 2006). The enzymes involved in this reaction in rats have not been identified. Cyp1a2, Cyp2d2, and Cyp4f1 were reported to catalyze CPD-0868 O-demethylation in rat liver microsomes (Generaux, 2010). In the current work, metabolic activity in rat SCH was maintained by supplementing the culture medium with 1 μM DEX, a standard concentration used in metabolism studies with SCH (Turncliff et al., 2006). Further studies are warranted to characterize the effect of DEX concentration on the expression/activity of the enzymes involved in the biotransformation of both prodrugs.

In summary, an integrated approach involving two rat hepatic systems (IPLs and SCH) and pharmacokinetic modeling provided a mechanistic understanding of the impact of hepatic binding on the systemic and hepatobiliary exposure of two antiparasitic active metabolites. As hypothesized, despite structural similarities, CPD-0868 had superior hepatobiliary disposition characteristics compared with pafuramidine, as reflected by more extensive formation of the active metabolite, CPD-0801, together with higher hepatic basolateral efflux (because of a higher hepatic unbound fraction), compared with furamidine. The combined effect of both factors could explain, in part, the enhanced systemic exposure of CPD-0801. Although the mechanisms of brain penetration for these active metabolites have not been elucidated, an increased systemic exposure of CPD-0801 could lead to improved brain exposure. Based on similar in vitro potencies of both active metabolites against various strains of trypanosomes (Wenzler et al., 2009), increased brain exposure of CPD-0801 may enhance antitrypanosomal efficacy in the central nervous system relative to furamidine. The agreement between results from rat IPLs and SCH further substantiates SCH as a useful in vitro tool for characterizing hepatobiliary disposition of xenobiotics. Because human IPLs are not feasible, human SCH could be used as a surrogate to predict hepatobiliary disposition of xenobiotics in humans.

Authorship Contributions

Participated in research design: Yan, Brouwer, and Paine.

Conducted experiments: Yan.

Performed data analysis: Yan, Brouwer, Pollack, Wang, Hall, and Paine.

Wrote or contributed to the writing of the manuscript: Yan, Brouwer, and Paine.

Other: Brouwer, Tidwell, Hall, and Paine acquired funding for the research.

References

Abe K, Bridges AS, Yue W, and Brouwer KL (2008) In vitro biliary clearance of angiotensin II receptor blockers and 3-hydroxy-3-methylglutaryl-coenzyme A reductase inhibitors in sandwich-cultured rat hepatocytes: comparison with in vivo biliary clearance. *J Pharmacol Exp Ther* **326:**983–990.

Barrett MP (2010) Potential new drugs for human African trypanosomiasis: some progress at last. *Curr Opin Infect Dis* **23:**603–608.

Boess F, Kamber M, Romer S, Gasser R, Muller D, Albertini S, and Suter L (2003) Gene expression in two hepatic cell lines, cultured primary hepatocytes, and liver slices compared to the in vivo liver gene expression in rats: possible implications for toxicogenomics use of in vitro systems. *Toxicol Sci* **73:**386–402.

Boykin DW, Kumar A, Hall JE, Bender BC, and Tidwell RR (1996) Anti-*Pneumocystis carinii* activity of bis-amidoximes and bis-*O*-alkylamidoxime prodrugs. *Bioorg Med Chem Lett* **6:**3017–3020.

Brouwer KL and Thurman RG (1996) Isolated perfused liver. *Pharm Biotechnol* **8:**161–192.

Generaux CN (2010) *Effects of Parasitic Infection on the Pharmacokinetics and Disposition of Pentamidine Analogs*. Ph.D. thesis, Eshelman School of Pharmacy, University of North Carolina, Chapel Hill.

Hewitt NJ, Lechón MJ, Houston JB, Hallifax D, Brown HS, Maurel P, Kenna JG, Gustavsson L, Lohmann C, Skonberg C, et al. (2007a) Primary hepatocytes: current understanding of the regulation of metabolic enzymes and transporter proteins, and pharmaceutical practice for the use of hepatocytes in metabolism, enzyme induction, transporter, clearance, and hepatotoxicity studies. *Drug Metab Rev* **39:**159–234.

Hewitt NJ, Lecluyse EL, and Ferguson SS (2007b) Induction of hepatic cytochrome P450 enzymes: methods, mechanisms, recommendations, and in vitro-in vivo correlations. *Xenobiotica* **37:**1196–1224.

Hoffmaster KA, Zamek-Gliszczynski MJ, Pollack GM, and Brouwer KL (2005) Multiple transport systems mediate the hepatic uptake and biliary excretion of the metabolically stable opioid peptide [D-penicillamine2,5]enkephalin. *Drug Metab Dispos* **33:**287–293.

Ismail MA and Boykin DW (2006) Synthesis of deuterium and ^{15}N-labelled 2,5-*Bis*[5-amidino-2-pyridyl]furan and 2,5-*Bis*[5-(methoxyamidino)-2-pyridyl]furan. *J Labelled Compounds Radiopharm* **49:**985–996.

Ismail MA, Brun R, Easterbrook JD, Tanious FA, Wilson WD, and Boykin DW (2003) Synthesis and antiprotozoal activity of aza-analogues of furamidine. *J Med Chem* **46:**4761–4769.

Ito K and Houston JB (2004) Comparison of the use of liver models for predicting drug clearance using in vitro kinetic data from hepatic microsomes and isolated hepatocytes. *Pharm Res* **21:**785–792.

Kienhuis AS, Wortelboer HM, Maas WJ, van Herwijnen M, Kleinjans JC, van Delft JH, and Stierum RH (2007) A sandwich-cultured rat hepatocyte system with increased metabolic competence evaluated by gene expression profiling. *Toxicol In Vitro* **21:**892–901.

LeCluyse EL (2001) Human hepatocyte culture systems for the in vitro evaluation of cytochrome P450 expression and regulation. *Eur J Pharm Sci* **13:**343–368.

LeCluyse EL, Audus KL, and Hochman JH (1994) Formation of extensive canalicular networks by rat hepatocytes cultured in collagen-sandwich configuration. *Am J Physiol Cell Physiol* **266:**C1764–C1774.

Lee JK, Leslie EM, Zamek-Gliszczynski MJ, and Brouwer KL (2008) Modulation of trabectedin (ET-743) hepatobiliary disposition by multidrug resistance-associated proteins (Mrps) may prevent hepatotoxicity. *Toxicol Appl Pharmacol* **228:**17–23.

Lee JK, Marion TL, Abe K, Lim C, Pollack GM, and Brouwer KL (2010) Hepatobiliary disposition of troglitazone and metabolites in rat and human sandwich-cultured hepatocytes: use of Monte Carlo simulations to assess the impact of changes in biliary excretion on troglitazone sulfate accumulation. *J Pharmacol Exp Ther* **332:**26–34.

Liu X, LeCluyse EL, Brouwer KR, Gan LS, Lemasters JJ, Stieger B, Meier PJ, and Brouwer KL (1999a) Biliary excretion in primary rat hepatocytes cultured in a collagen-sandwich configuration. *Am J Physiol Gastrointest Liver Physiol* **277:**G12–G21.

Liu X, LeCluyse EL, Brouwer KR, Lightfoot RM, Lee JI, and Brouwer KL (1999b) Use of Ca^{2+} modulation to evaluate biliary excretion in sandwich-cultured rat hepatocytes. *J Pharmacol Exp Ther* **289:**1592–1599.

Midgley I, Fitzpatrick K, Taylor LM, Houchen TL, Henderson SJ, Wright SJ, Cybulski ZR, John BA, McBurney A, Boykin DW, et al. (2007) Pharmacokinetics and metabolism of the prodrug DB289 (2,5-bis[4-(*N*-methoxyamidino)phenyl]furan monomaleate) in rat and monkey and its conversion to the antiprotozoal/antifungal drug DB75 (2,5-bis(4-guanylphenyl)furan dihydrochloride). *Drug Metab Dispos* **35:**955–967.

Paine MF, Wang MZ, Generaux CN, Boykin DW, Wilson WD, De Koning HP, Olson CA, Pohlig G, Burri C, Brun R, et al. (2010) Diamidines for human African trypanosomiasis. *Curr Opin Investig Drugs* **11:**876–883.

Pang KS, Lee WF, Cherry WF, Yuen V, Accaputo J, Fayz S, Schwab AJ, and Goresky CA (1988) Effects of perfusate flow rate on measured blood volume, disse space, intracellular water space, and drug extraction in the perfused rat liver preparation: characterization by the multiple indicator dilution technique. *J Pharmacokinet Biopharm* **16:**595–632.

Pang KS, Morris ME, and Sun H (2008) Formed and preformed metabolites: facts and comparisons. *J Pharm Pharmacol* **60:**1247–1275.

Pessayre D, Mansouri A, Haouzi D, and Fromenty B (1999) Hepatotoxicity due to mitochondrial dysfunction. *Cell Biol Toxicol* **15:**367–373.

Rowland M (1985) Physiologic pharmacokinetic models and interanimal species scaling. *Pharmacol Ther* **29:**49–68.

Swift B, Pfeifer ND, and Brouwer KL (2010) Sandwich-cultured hepatocytes: an in vitro model to evaluate hepatobiliary transporter-based drug interactions and hepatotoxicity. *Drug Metab Rev* **42:**446–471.

Turncliff RZ, Hoffmaster KA, Kalvass JC, Pollack GM, and Brouwer KL (2006) Hepatobiliary disposition of a drug/metabolite pair: Comprehensive pharmacokinetic modeling in sandwich-cultured rat hepatocytes. *J Pharmacol Exp Ther* **318:**881–889.

Wang MZ, Saulter JY, Usuki E, Cheung YL, Hall M, Bridges AS, Loewen G, Parkinson OT, Stephens CE, Allen JL, et al. (2006) CYP4F enzymes are the major enzymes in human liver microsomes that catalyze the O-demethylation of the antiparasitic prodrug DB289 [2,5-bis(4-amidinophenyl)furan-bis-*O*-methylamidoxime]. *Drug Metab Dispos* **34:**1985–1994.

Wenzler T, Boykin DW, Ismail MA, Hall JE, Tidwell RR, and Brun R (2009) New treatment option for second-stage African sleeping sickness: in vitro and in vivo efficacy of aza analogs of DB289. *Antimicrob Agents Chemother* **53:**4185–4192.

Wu H, Ming X, Wang MZ, Tidwell R and Hall JE (2007) Comparative pharmacokinetics of the antitrypanosomal diamidines DB75, DB820 and DB829 following oral administration of their dimethamidoximes prodrugs in mice. *AAPS J* **9(S2):** W4402.

Zhou L, Thakker DR, Voyksner RD, Anbazhagan M, Boykin DW, Hall JE, and Tidwell RR (2004) Metabolites of an orally active antimicrobial prodrug, 2,5-bis(4-amidinophenyl)furan-bis-*O*-methylamidoxime, identified by liquid chromatography/tandem mass spectrometry. *J Mass Spectrom* **39:**351–360.

Address correspondence to: Dr. Mary F. Paine, UNC Eshelman School of Pharmacy, 2320 Kerr Hall, CB 7569, University of North Carolina, Chapel Hill, NC 27599-7569. E-mail: mpaine@unc.edu